

## Controlled underdoping of cuprates using ultraviolet radiation

P. Schwaller, S. Berner, T. Greber, and J. Osterwalder  
 Physik-Institut der Universität Zürich, CH-8057 Zürich, Switzerland

H. Berger  
 Institut de Physique Appliquée, EPFL, CH-1015 Lausanne, Switzerland

(Received 28 September 1998; accepted for publication 2 February 1999)

A method for a controlled change of the doping level of high-temperature superconductors with ultraviolet radiation is presented. With photoemission it is shown that the exposure of  $\text{Bi}_2\text{Sr}_2\text{CaCu}_2\text{O}_{8+\delta}$  samples to the light of a He gas-discharge lamp causes oxygen desorption. From measurements of the Fermi surface, it is found that the oxygen desorption causes a decrease of the doping level of the superconductors. From the desorption cross sections that strongly depend on the photon energy, two different oxygen desorption channels are inferred. This procedure for decreasing the doping level has the advantage that the crystallinity of the sample is not altered and that the doping level can be simultaneously measured by photoelectron spectroscopy. © 1999 American Institute of Physics. [S0003-6951(99)03713-4]

Applications of high-temperature superconductors critically depend on the quality of these materials. Today it is state of the art to produce homogeneous single-crystal samples at various doping levels, i.e., with various superconducting transition temperatures  $T_c$ . However, it may be important to produce well-defined lateral structures between superconducting, and nonsuperconducting zones or regions with a gradual  $T_c$  on *one* thin cuprate layer. It is, therefore, essential to develop tools for the tailoring of such structures. For example, it is reported that Josephson junctions on  $\text{YBa}_2\text{Cu}_2\text{O}_{7-\delta}$  can be fabricated by electron-beam writing.<sup>1</sup> Or, that  $\text{YBa}_2\text{Cu}_2\text{O}_{7-\delta}$  films are patterned by a procedure based on a local increase of the oxygen diffusion velocity that is increased by the heat of a focused laser beam.<sup>2</sup> Here, we suggest that such structures could be fabricated by the exposure of high-temperature superconductors to ultraviolet (UV) radiation.

This letter describes a controlled reduction of the oxygen content within the surface region of single-crystalline  $\text{Bi}_2\text{Sr}_2\text{CaCu}_2\text{O}_{8+\delta}$  (Bi2212) by UV radiation. The process works at room temperature and maintains the crystallinity of the sample. In Bi-type cuprates oxygen loss is equivalent to a reduction of the hole concentration and, thus, to a change of  $T_c$ .<sup>3,4</sup> A further advantage of using UV radiation to change the doping level is that the sample modifications can be *simultaneously* measured by ultraviolet photoelectron spectroscopy (UPS) that uses the same UV radiation which is applied for the doping level modification.

The experiments were performed in a VG ESCALAB 220 photoelectron spectrometer. It is equipped with a custom-made two-axis sample goniometer which allows computer-controlled angle-resolved photoemission measurements.<sup>5</sup> The high-intensity UV radiation is produced in a Gammadata helium electron cyclotron resonance (ECR) plasma lamp. The line spectrum of the lamp is monochromatized by a toroidal grating. The monochromator has been used in three different settings: zeroth-order, first-order He I $\alpha$  (21.2 eV photon energy), and first-order He II $\alpha$  (40.8 eV) radiation. Typical flux values (in  $10^{10}$  photons/mm<sup>2</sup> s) on a

spot of about 7 mm<sup>2</sup> are 178 (He I<sup>0.order</sup>), 3.62 (He II<sup>0.order</sup>), 69.9 (He I $\alpha$ ), and 9.4 for He II $\alpha$ . The growth of the Bi2212 crystals and their preparation for the photoemission experiments are described in Refs. 6 and 7.

Figure 1 shows normal emission He I spectra near the Fermi level of high  $T_c$  superconductors at room temperature. Spectra of an optimally doped Bi2212 single crystal ( $T_c = 84$  K, hole concentration  $x=0.185$ ) and of a strongly underdoped  $\text{Pr}_{0.05}\text{Bi}_2\text{Sr}_2\text{Ca}_{0.95}\text{Cu}_2\text{O}_{8+\delta}$  (Pr-Bi2212) sample ( $T_c = 30$  K,  $x=0.07$ ), both measured shortly after cleaving in ultrahigh vacuum, are plotted in Fig. 1(a). In order to compare the data from two different sample surfaces, the two spectra are scaled to the same intensity at 500 meV binding energy. The spectral weight of normal emission from the Fermi level is below 2% of the maximum intensity in the valence band and about 20% compared to a location on the Fermi surface. The normal emission from the Fermi level stems from indirect transitions since it probes no Fermi surface location; nevertheless it is a mean for the quantification

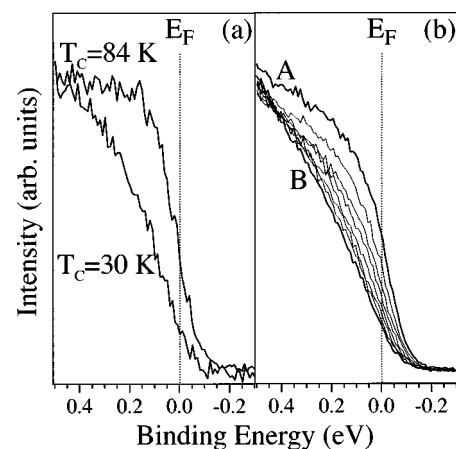


FIG. 1. (a) Normal emission He I spectra of optimally doped  $\text{Bi}_2\text{Sr}_2\text{CaCu}_2\text{O}_{8+\delta}$  (Bi2212) and underdoped  $\text{Pr}_{0.05}\text{Bi}_2\text{Sr}_2\text{Ca}_{0.95}\text{Cu}_2\text{O}_{8+\delta}$  (Pr-Bi2212). The spectra are scaled to the same intensity at 500 meV binding energy. (b) Evolution of the leading edge of optimally doped Bi2212 as a function of the He I exposure.

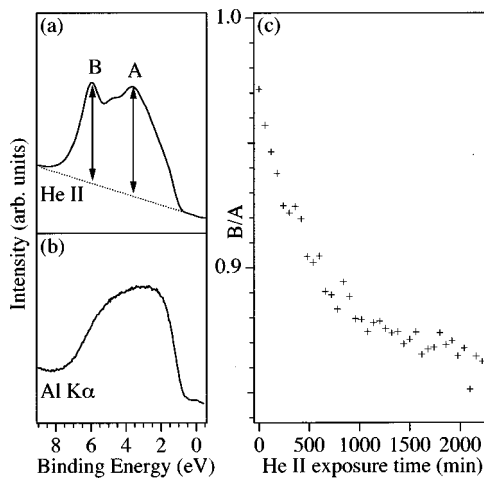


FIG. 2. Valence-band spectra of optimally doped Bi2212 (a) measured using He II UV radiation and (b) Al  $K\alpha$  x rays. (c) Relative intensity of the oxygen-related peak B as a function of He II exposure.

of the effect of UV radiation that is reported in this letter. Figure 1(b) depicts spectra around  $E_F$  for optimally doped Bi2212 as a function of the He I exposure. At low exposure (spectrum A) the leading edge at  $E_F$  is clearly visible. With increasing exposure the spectral weight at  $E_F$  drops and the leading edge vanishes. After an exposure of  $7.4 \times 10^{16}$  photons/mm<sup>2</sup> (spectrum B), the shape of the spectrum is similar to that of a strongly underdoped Bi2212 sample [see Fig. 1(a)]. Upon annealing the sample to 450 K the loss of spectral weight partially recovers. Further experiments showed that the loss rate of spectral weight at the Fermi level is proportional to the UV light flux.

The behavior described above suggests that the charge-carrier concentration of the Bi2212 sample can be decreased by UV radiation. This effect is different from an aging effect reported by Ding *et al.*<sup>8</sup> They observed an underdoped sample become more doped during their experiments at low temperature. Our effect is induced by UV radiation at 300 K and is observed on initially optimally doped samples that are stable under UHV conditions.<sup>7</sup> In Bi2212 a reduction of the charge-carrier concentration can be realized by a reduction of the oxygen concentration. In order to corroborate the hypothesis that the UV light reduces the oxygen content, an oxygen spectral feature has been recorded as a function of UV light exposure. O2*p* related features in the valence band (VB) have been identified using photoemission cross-section ratios between UV and x-ray energies. The cross-section ratio  $\sigma[\text{O}2p(\text{He II})]:\sigma[\text{O}2p(\text{Al } K\alpha)]$  is  $2.8 \times 10^4$  and more than one order of magnitude larger than the corresponding ratios for all other components in the valence band. Thus, oxygen features should be visible in He II VB spectra and should be suppressed in Al  $K\alpha$  excited VB spectra. Figures 2(a) and 2(b) show VB spectra of optimally doped Bi2212 measured with He II and Al  $K\alpha$ , respectively. The He II spectrum has been convoluted with a Gaussian with 500 meV full width at half maximum (FWHM) in order to have the same energy resolution in both spectra. In the He II spectrum two peaks at 3.5 eV (peak A) and at 6 eV (peak B) binding energy are observed. Peak B has high intensity in the He II spectrum but is absent in the Al  $K\alpha$  measurement. From this and the O2*p* cross-section ratio, one can conjecture that peak B is mainly

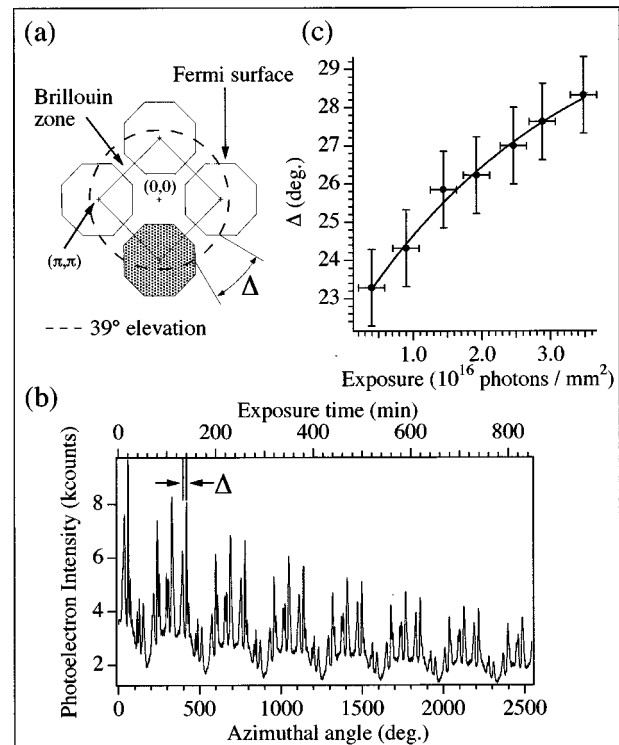


FIG. 3. (a) Schematic drawing of the Fermi surface of optimally doped Bi2212. (b) Evolution of the photoelectron intensity at  $E_F$  at 39° polar emission angle (elevation) as a function of the azimuthal angle and of the He I exposure. (c) Evolution of  $\Delta$  with He I exposure.

related to O2*p* states. Peak A served for normalization purposes.

Figure 2(c) shows the peak intensity ratio between peaks B and A as a function of He II exposure time. The decrease of this ratio evidences that the oxygen content is reduced due to the UV radiation. From the decrease of the B:A ratio by about 15% it cannot be concluded that the oxygen content decreases by this amount since, e.g., not all oxygen atoms in the Bi2212 structure have to contribute to peak B.

The measurements of spectra near  $E_F$  (Fig. 1) revealed that UV radiation reduces the charge-carrier concentration. This must be reflected in the Fermi surface (FS) that is shrinking upon underdoping the Bi2212 samples.<sup>7-11</sup> This issue is depicted in Fig. 3(a) where a schematic drawing of the situation in  $\mathbf{k}$  space is shown. The FS consists of barrels (here, approximated by regular octagons) centered at the  $(\pi, \pi)$  points in reciprocal space. The FS volume is, in our case, equal to the grey area of one FS barrel around  $(\pi, \pi)$ . The FS intersection angle  $\Delta$  [see Fig. 3(a)] is a measure for the FS volume.

To investigate the influence of UV radiation on the FS volume, an optimally doped Bi2212 sample has been exposed to He I radiation and  $\Delta$  has been simultaneously monitored. For each azimuthal step at the polar emission angle of 39° off normal, the total photoelectron intensity centered at  $E_F$  has been measured with an energy resolution of 100 meV FWHM. High photoelectron intensity in this analyzer setting is equivalent to photoemission from the Fermi surface.<sup>7,12</sup> The result of such a multiple azimuthal scan with a continuously increasing He I exposure is shown in Fig. 3(b). Each peak corresponds to photoemission from the FS and the FS

intersection angles  $\Delta$  can be determined. The decrease of the photoelectron intensity is explained by the reduction of the intensity at  $E_F$  due to the UV radiation [see Fig. 1(b)]. The periodic intensity dip is attributed to an inhomogeneity of this specific cleaved surface.

Figure 3(c) shows the behavior of the FS intersection angle  $\Delta$  as a function of the He I exposure. Each data point is the average of the four  $\Delta$  values obtained from a 360° azimuthal scan. At low exposure,  $\Delta_0$  corresponds to the value previously found for optimally doped Bi2212.<sup>7</sup> According to what one expects for a reduced hole concentration,  $\Delta$  increases (i.e., the FS is shrinking) with increasing UV exposure. The solid line in Fig. 3(c) corresponds to the first-order kinetics of the form  $\Delta = \Delta_\infty - (\Delta_\infty - \Delta_0)e^{-t/\tau}$ , where  $1/\tau$  is the shrinking rate,  $\Delta_0$  the initial intersection angle, and  $\Delta_\infty$  the saturation value. It is remarkable that  $\Delta_\infty(31^\circ \pm 2^\circ)$  coincides with the  $\Delta$  value found for a strongly underdoped Pr-Bi2212 sample ( $T_c = 30$  K, hole concentration  $x = 0.07$ ). This suggests again that the excess (doping) oxygen that renders the material conducting is removed from the  $\text{Bi}_2\text{Sr}_2\text{CaCu}_2\text{O}_{8+\delta}$  structure. Apparently, the photodesorption of nondoping oxygen is not efficient. We would like to emphasize that even after a high UV exposure, dispersion is clearly visible [see Fig. 3(b)]. This indicates that the crystallinity of Bi2212 single crystals is not destroyed due to the UV radiation. The spectral features near the Fermi level are most sensitive to the doping, and thus to the oxygen content of the sample. The increase of  $\Delta$  by  $8^\circ$  corresponds to a decrease in oxygen content of about 2%. Therefore, relative variations in the oxygen content of 0.2% in the surface region can readily be measured.

Now the photon energy dependence of the UV-doping cross sections will be briefly discussed. For this, optimally doped Bi2212 samples have been exposed in succession to zeroth-order He radiation, monochromatized He II, and monochromatized He I radiation, and the intensity at  $E_F$  for normal photoelectron emission has been determined.<sup>13</sup> This intensity decreases with UV exposure (see Fig. 1), as does the oxygen content (see Fig. 2), and as the Fermi surface shrinks (see Fig. 3). The shrinking rate  $1/\tau$  equals  $\phi\sigma$ , where  $\phi$  is the photon flux and  $\sigma$  the desorption cross section. The desorption cross-sections  $\sigma_{\text{He I}}$  and  $\sigma_{\text{He II}}$  are thus determined from the rate measurements and the corresponding photon fluxes. We find desorption cross sections of  $188 \pm 53$  kb for He II and  $23 \pm 6$  kb for He I radiation ( $1 \text{ b} = 10^{-24} \text{ cm}^2$ ). The relatively large error bars result from the uncertainties in the photoionization cross-section values of Cairns and Samson,<sup>14</sup> which are used to quantify the photon fluxes  $\phi$ . Note that the shrinking rates of the data in Figs. 2 and 3 are consistent with these desorption cross sections.

Finally, we would like to discuss a model for the UV-doping process that comprises the light-induced oxygen desorption from the near-surface region of Bi2212. The surface of Bi2212 is terminated by a Bi-O layer.<sup>15</sup> Therefore, only oxygen originating from the Bi-O surface layer can directly leave the crystal by photodesorption. The UV-doping process is thus expected to be limited to the near-surface region even if, after a (partial) oxygen depletion of the surface layer, oxygen diffusion from deeper charge reservoir planes to the surface is possible.

The details of the photodesorption process are not clear at the moment. The process has, however, included an electronic excitation that leads to acceleration and possible desorption of oxygen atoms.<sup>16</sup> At first, it is most likely that a process like  $\text{O}2p^6 + \hbar\omega \rightarrow \text{O}2p^5 + e_{\text{photo}}$  could force the  $\text{O}^-$  ion on  $\text{O}^{2-}$ -like sites to desorption. However, the experimental finding that the UV-doping process is much more efficient using He II radiation indicates more than one desorption mechanism. From the photodesorption cross sections of He II (188 kb) and He I radiation (23 kb), we conjecture that not only  $\text{O}2p$  photoexcitation, where the photoemission cross sections are 6.8 and 10.7 Mb, respectively, leads to desorption. In fact, we speculate that the photoexcitation of  $\text{O}2s$  levels that are reached by He II radiation ( $\sigma_{\text{photo}} = 834$  kb) opens a very efficient desorption channel that produces neutral oxygen atoms via a process like  $\text{O}2s^22p^6 + \hbar\omega \rightarrow \text{O}2s^12p^6 + e_{\text{photo}} \rightarrow \text{O}2s^22p^4 + e_{\text{Auger}}$  from  $\text{O}^{2-}$ -like ions. These neutrals are expected to be accelerated more effectively away from the surface than the ions. Clearly, experiments with tunable UV radiation could shed more light on the details of the photodesorption process of oxygen from ceramic materials.

In summary we have shown that it is possible to change, continuously the doping level within the surface region of Bi2212 by UV radiation. The UV-doping technique has the advantage that sample modifications can be simultaneously monitored using photoelectron spectroscopy. Furthermore, we have shown that the technique does not destroy the crystallinity of the samples. Using thin films, this technique could be applied to the fabrication of microelectronic devices built from high-temperature superconductors.

The authors would like to thank F. Bourqui, W. Deichmann, O. Raetz, B. Schmid, and P. Treier for skillful technical assistance. This work was supported by the Swiss National Science Foundation.

<sup>1</sup>B. M. Hinaus, M. S. Rzechowski, B. A. Davidson, J. E. Nordman, K. Siangchaew, and M. Libra, *Phys. Rev. B* **56**, 1 (1997).

<sup>2</sup>J. Eisenmenger, C. Brand, and P. Leiderer, *Physica C* **262**, 168 (1996).

<sup>3</sup>For an introduction to superconductivity, see M. Cyrot and D. Pavuna, *Introduction to Superconductivity and High  $T_c$  Materials* (World Scientific, Singapore, 1992).

<sup>4</sup>W. A. Groen, D. M. de Leeuw, and L. F. Feiner, *Physica C* **165**, 55 (1990).

<sup>5</sup>T. Greber, O. Raetz, T. J. Kreuz, P. Schwaller, W. Deichmann, E. Wetli, and J. Osterwalder, *Rev. Sci. Instrum.* **68**, 4549 (1997).

<sup>6</sup>A. B. Bykov and L. N. Demmianets, *J. Cryst. Growth* **139**, 81 (1994).

<sup>7</sup>P. Schwaller, Ph.D. thesis, University of Zürich (1997).

<sup>8</sup>H. Ding, M. R. Norman, T. Yokoya, T. Takeuchi, M. Randeira, J. C. Campuzano, T. Takahashi, T. Mochiku, and K. Kadowaki, *Phys. Rev. Lett.* **78**, 2628 (1997).

<sup>9</sup>D. S. Dessau, D. S. Marshall, A. G. Loeser, C.-H. Park, A. Y. Matsuura, Z.-X. Shen, P. Fournier, A. Kapitulnik, K. Kishio, J. Eckstein, and I. Bozovic, *J. Electron Spectrosc. Relat. Phenom.* **78**, 167 (1996).

<sup>10</sup>I. Vobornik, S. La Rosa, F. Zwick, H. Berger, M. Griani, G. Margaritondo, R. J. Kelley, J. Ma, A. Chubukov, and M. Onellion, *Helv. Phys. Acta* **69**, 225 (1996).

<sup>11</sup>H. Ding, T. Yokoya, J. C. Campuzano, T. Takahashi, M. Randeria, M. R. Norman, T. Mochiku, K. Kadowaki, and J. Giapintzakis, *Nature (London)* **382**, 51 (1996).

<sup>12</sup>P. Aebi *et al.*, *Phys. Rev. Lett.* **72**, 2757 (1994).

<sup>13</sup>S. Berner, Diploma thesis, University of Zürich (1998).

<sup>14</sup>R. B. Cairns and J. A. R. Samson, *J. Opt. Soc. Am.* **56**, 1568 (1966).

<sup>15</sup>M. Shimoda, T. Greber, J. Osterwalder, and L. Schlappbach, *Physica C* **196**, 236 (1992).

<sup>16</sup>P. Avouris and R. E. Walkup, *Annu. Rev. Phys. Chem.* **40**, 173 (1989).